CONF-900563--17

DE91 004630

DEC 0 4 1990

A LOGARITHMIC, LARGE-SOLID-ANGLE DETECTOR TELESCOPE FOR NUCLEAR FRAGMENTATION

K. KWIATKOWSKI, K. KOMISARCIK, J.L. WILE, S.J. YENNELLO, D.E. FIELDS AND V.E. VIOLA
Departments of Chemistry and Physics and IUCF, Indiana University, Bloomington, IN 47405

B.G. GLAGOLA
Physics Division, Argonne National Laboratory, Argonne, IL 60439

Properties of a logarithmic, large-solid-angle detector telescope for measuring the spectra of light charged particles and/or complex fragments produced in intermediate-energy nuclear reactions are described. Light-ion identification with a phoswich detector which consists of transmission photodiode ΔE and CsI(Tℓ) E elements is also discussed, as is the response of silicon microstrip detectors to fission fragments.

1. Introduction

The investigation of hot nuclear matter formed in central collisions between intermediate-energy projectiles and heavy target nuclei demands a highly versatile detector system. This condition is imposed by the complex spectrum of fragments produced in such collisions--which span a broad range in mass, charge and kinetic energy [1]. At the same time, the multibody nature of these events is such that determination of fragment multiplicities and spatial relationships on an event-by-event basis is essential for understanding the salient reaction mechanisms. Thus, full solid-angle coverage with good granularity is a prerequisite for such studies.

In this paper we discuss the features of several particle identification telescopes based upon passivated silicon or photodiode technology that have been developed for use in a multi-element detector system for the study of

DISCLAIMER

fragmentation reactions at intermediate energies.

2. Logarithmic Detector

The detector described here has been designed to measure the spectra of light-charged particles (LCP = H and He) up to energies of ≈ 70 MeV/nucleon and intermediate-mass fragments (IMF: $Z \leq 3 \lesssim 15$) emitted in central collisions at intermediate bombarding energies. Reported here are the properties of a detector telescope with an active area of 25 cm^2 which consists of the following elements: (1) a gas-ionization counter, (2) two passivated silicon detectors, and (3) two CsI(Tℓ) scintillator crystal operated with photodiodes. A cross-sectional diagram of the detector is shown in Fig. 1.

The gas-ionization counter (GIC) element is of the axial field design and is operated at 15-20 Torr of CF_4 gas. In order to minimize the electron collection time, the anode plane is positioned in the middle of the active length of the ion chamber. The anode consists of a square brass frame with 12 parallel, gold-plated tungsten wires of 50 μm diameter strung across the frame. Each wire spacing is 3.8 mm. To ensure the uniformity of the electric field, three field-shaping electrodes are placed on each side of the collector electrode. This detector provides energy-loss, ΔE, information for charge identification of Z ≥ 3 fragments with good charge resolution. The pair of 5 cm x 5 cm silicon (Si) detectors [2], with thicknesses of 220 μm and 500 μm, respectively, serve several functions. The 200 μm element provides energy information for ΔE-E charge identification of low-energy and/or massive fragments. When combined with an appropriate fast start signal, e.g. a beam RF signal, the detector also provides a fast-timing stop signal for time-of-flight (TOF) mass determinations of all fragments stopped in the detector. By removing gas from the GIC, the front silicon detector can also be used for recoil or fission fragment TOF mass identification. The high degree of uniformity of the 220 μm and 500 μm silicon elements permits charge and mass identification of fragments up to oxygen, which stop in the 500 μm detector.

The scintillation detector consists of a pair of 1.7 cm thick x 2.8 cm x 5.6 cm (front-face area) CsI(Tℓ) crystals operated side-by-side, with a pair of 2 cm x 1 cm photodiodes glued to the top and the bottom of each crystal [3]. The two photodiodes are connected in parallel to a Canberra 2004 preamplifier. These elements are capable of stopping up to ~70 MeV/nucleon hydrogen and helium ions with good isotopic resolution. An added advantage of the operation of CsI(Tℓ) crystals in conjunction with silicon detectors is relative ease and reliability of calibrating the scintillator light output based upon the known energy response of silicon semiconductors.

Tests of this device have been performed at the Argonne National Laboratory ATLAS accelerator with 160-MeV ^{16}O ions incident on a ^{nat}Ag target. Figures 2(a), (b) and (c) show the respective charge identification spectra for fragments observed at 20° in the laboratory system for each successive pair of detector $\Delta E/E$ elements (i.e., GIC/220 μm Si; 220μm Si/500 μm Si; and 500 μm Si/17 mm CsI(Tl)). Figure 2(d) displays a time-of-flight versus energy spectrum for TOF derived from the 220 μm detector and the ATLAS linac booster RF signal (~ 200 ps timing resolution). A rise time of $\tau_R \approx 10.5$ ns was obtained with a fast time pickoff unit [4] and 40% overbias on the detector, providing a timing resolution of 300 ps (excluding the beam contribution) for elastic ^{16}O ions. Figures 3(a) and (b) show the respective mass and charge projections for the detector, integrated over all fragment energies above ~ 0.3 MeV/nucleon. The charge and mass resolution are about 0.3-0.4 units each, yielding excellent nuclide resolution for all projectile-like products of this reaction.

Detectors of this design have subsequently been used for studies of E/A = 60-100 MeV ^{14}N-induced reactions at the National Superconducting Cyclotron Laboratory at Michigan State University and with 0.9-6 GeV ^{3}He beams at the Laboratoire National Saturne in Saclay and at the LBL Bevalac. Thus far, they have shown excellent long-term stability and lifetime when placed in vacuum and exposed to such beams for periods of over one week.

In order to reduce cost, it may be advantageous to operate the telescope with a single thin silicon detector, or possibly in an ion chamber/CsI(Tℓ) configuration. In such cases energetic LCP identification can be accomplished via pulse shape analysis [5]. Fig. 4 shows a scatter plot of LCP identification obtained with bipolar pulses and a zero-crossing discriminator. Excellent particle identification resolution can be observed up to the punch-through energies. Recently, comparable results were obtained with a more compact design of a CsI(Tℓ) detector (5.6 cm x 5.6 cm x 2 cm) with a single 1.8 cm x 1.8 cm photodiode [3] mounted on an axial light guide.

3. Photodiode Phoswich

A novel type of ΔE/E phoswich detector has also been tested. This device employs a 1 cm x 1 cm, 307-μm thick fully-depleted photodiode [6] mounted in a transmission holder and glued directly to the front face of a 2.6 cm long CsI(Tℓ) crystal with Ecobond 24 epoxy. In this mode the photodiode serves simultaneously as a silicon ΔE counter via its fast output and as the light detector for the slow 560 nm light signal from the CsI(Tℓ) scintillator. The fast signal was derived by differentiation of the preamplifier (Canberra 2004 and Ortec H242A) signals with a timing-filter amplifier. This device provides the advantage of readout-element simplification via the phoswich technique and scintillator calibration via the known Si detector response. This device has recently been tested with 270-MeV ^3He beams incident on a mylar target at the Indiana University Cyclotron Facility. Fig. 5 presents a spectrum for the phoswich with the photodiode glued to the front face of the CsI(Tℓ); here the fast photodiode output is plotted versus the total light output of the photodiode/CsI(Tℓ) pair. Good particle-identification resolution is observed; the lower diagonal line corresponds to particles which stop in the silicon element.

4. Silicon Microstrip Detection of Fission Fragments

In order to provide a better definition of the angular correlations between fission fragments and to measure heavy recoil fragment masses produced in intermediate-energy collisions, the use of an array of 6 cm x 4 cm segmented silicon microstrip detectors with 2 mm strips [2] for a fission-fission coincidence trigger has also been investigated. Position sensitivity is obtained via charge division in a network of 10 ohm resistors; a position spectrum is shown in Fig. 6 for a 28-strip, 300-μm detector. The response of individual strips to a ^{252}Cf spontaneous fission source provides spectra which satisfy the criteria of surface barrier detectors established by Schmitt and Pleasanton [7]. This indicates relatively small dead layers on these detectors, thus enabling energy-energy correlation measurements. The best rise time for detectors tested with fission fragments thus far is approximately 16 nsec.

We wish to acknowledge valuable discussions with Dr. V. Rauch (CRN, Strasbourg) concerning the design of axial ion chambers. Work supported by the U. S. Department of Energy, Nuclear Physics Division, under Contract W-31-109-ENG-38.

<u>References</u>

1. <u>Proc. Symposium on Nucl. Dynamics and Nucl. Disassembly</u>, J.B. Natowitz, ed. (World Scientific, Singapore, 1989).

2. Series MSX 25 and design J detectors, Micron Semiconductor, Ltd., Lancing, Sussex, ENGLAND.

3. Hamamatsu Corp., Bridgewater, NJ; K. Yamamoto et al., Nucl. Instr. Meth. A253 (1987) 542.

4. H. Spieler, LBL timing preamplifier 21X 742, IEEE Trans. Nucl. Science, NS-29 (1982) 1142.

5. P. Kreutz et al., Nucl. Instr. Meth. A260 (1987) 120.

6. Custom order from Micron Semiconductor.

7. H.W. Schmitt and F. Pleasanton, Nucl. Instr. Meth. 40 (1966) 204.

Figure Captions

Fig. 1 Schematic diagram of large-solid-angle, logarithmic complex-fragment/light-charged-particle detector telescope. Legend: A - anode; W - 1.5 μm thick aluminized mylar window; F - field shaping electrode; S - silicon detectors; C - CsI(Tℓ) scintillator, and PD - photodiodes.

Fig. 2 (a) Particle identification spectrum for gas-ion chamber versus 220 μm silicon detector; (b) same for 220 μm silicon vs. 500 μm silicon detector; (c) same for 500 μm vs. CsI detector with two photodiodes readout, and (d) time-of-flight relative to beam RF vs. fragment energy.

Fig. 3 Spectrum of (a) atomic number and (b) mass number for all fragments (except protons above 70 MeV) for 160-MeV ^{16}O + ^{197}Au reaction at 20°.

Fig. 4 Scatter plot of pulse-shape discrimination TAC output versus light output of the CsI(Tℓ) detector.

Fig. 5 Raw nuclide identification for H and He isotopes using a transmission mounted photodiode glued to the front face of a CsI(Tℓ) crystal. Vertical axis shows the fast output from the photodiode; horizontal axis is the total integrated output from both the photodiode and CsI(Tℓ) crystal with the fast signal subtracted out.

Fig. 6 Positron spectrum for 28-strip detector of area 6 cm x 4 cm observed in reaction of 135-MeV protons with ^{238}U gated on fission fragments.

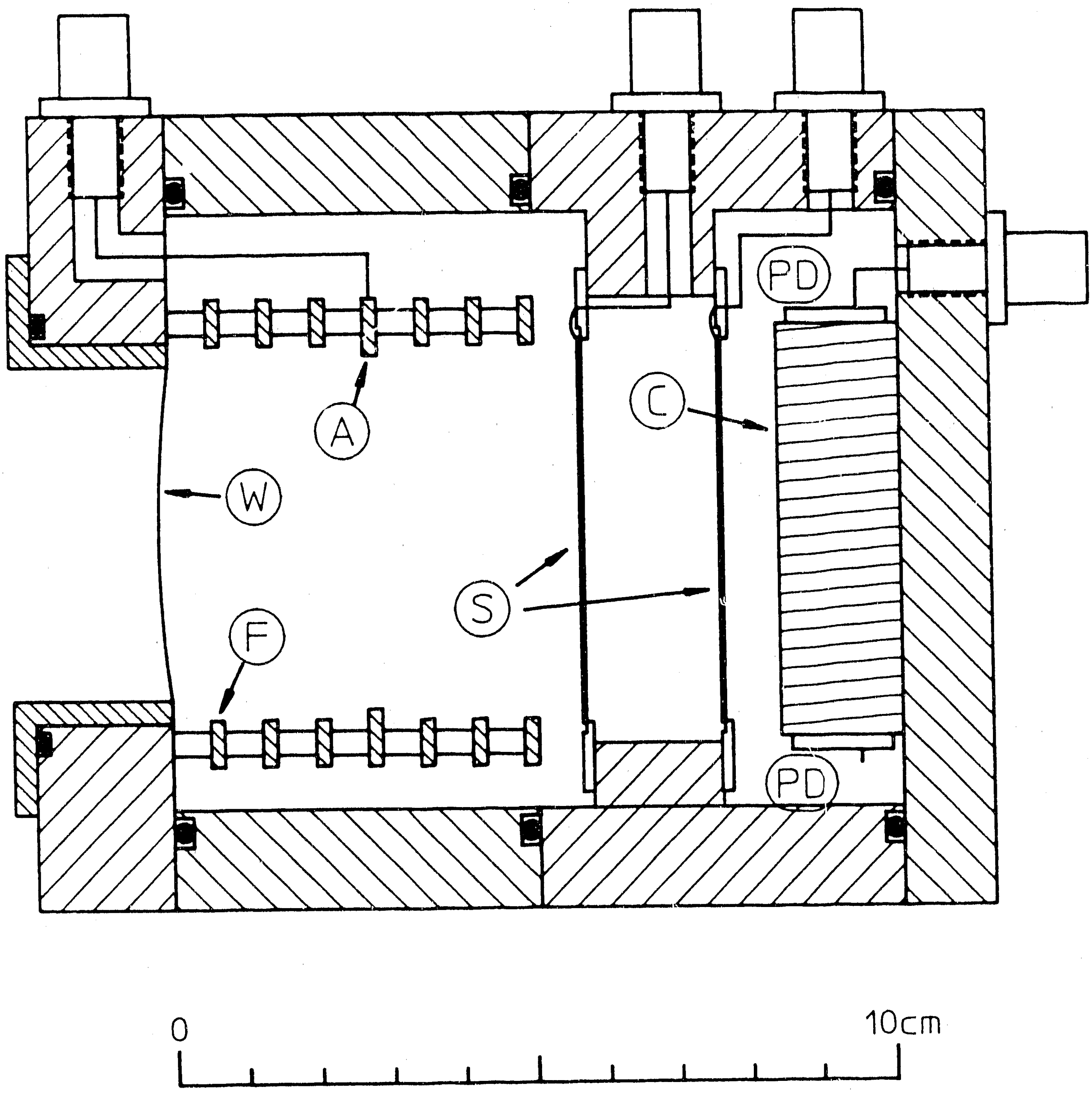

Fig. 1

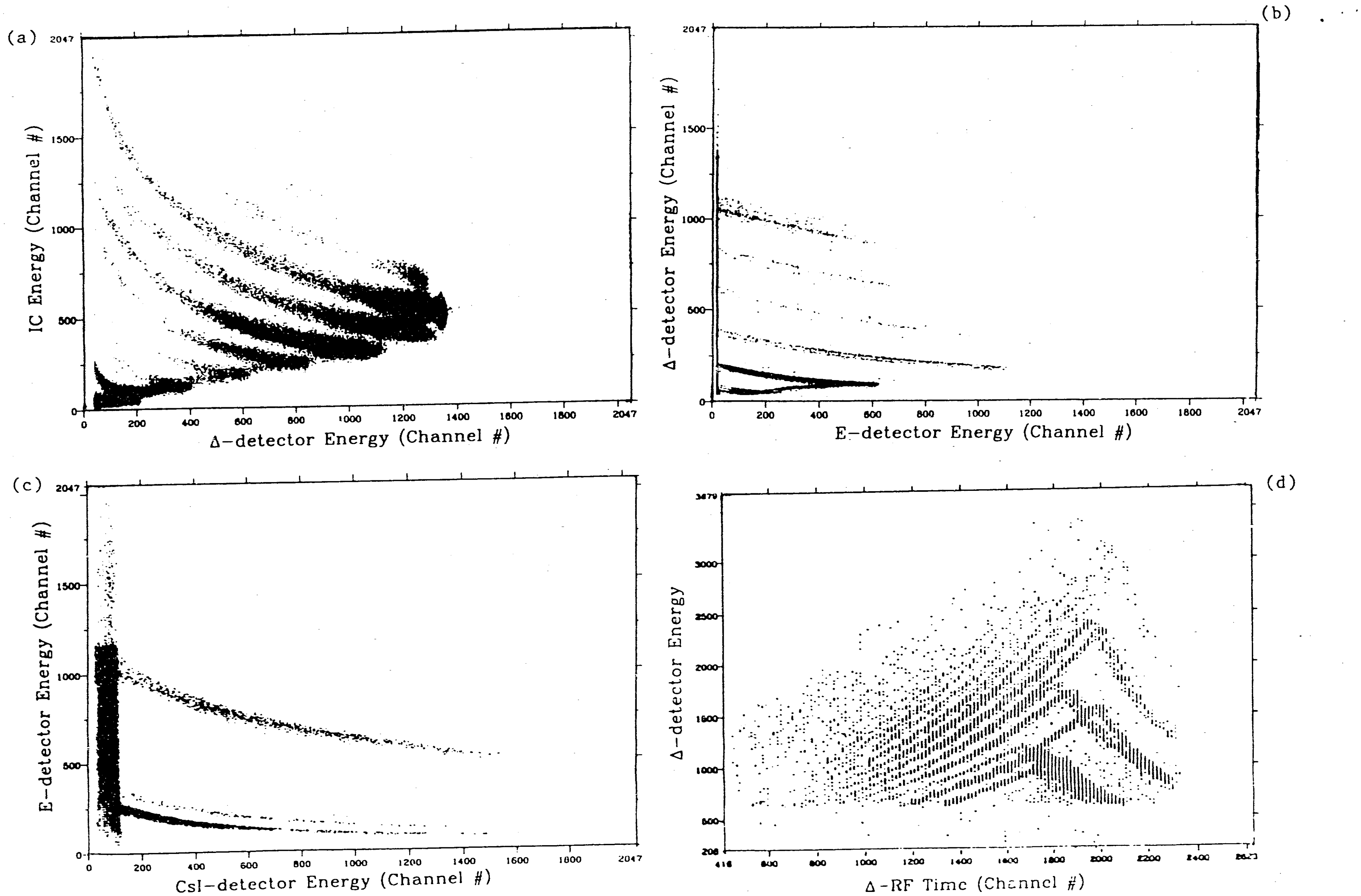
(a)
IC Energy (Channel #)
Δ-detector Energy (Channel #)
(b)
Δ-detector Energy (Channel #)
E-detector Energy (Channel #)
(c)
E-detector Energy (Channel #)
CsI-detector Energy (Channel #)
(d)
Δ-detector Energy
Δ-RF Time (Channel #)

Fig. 2

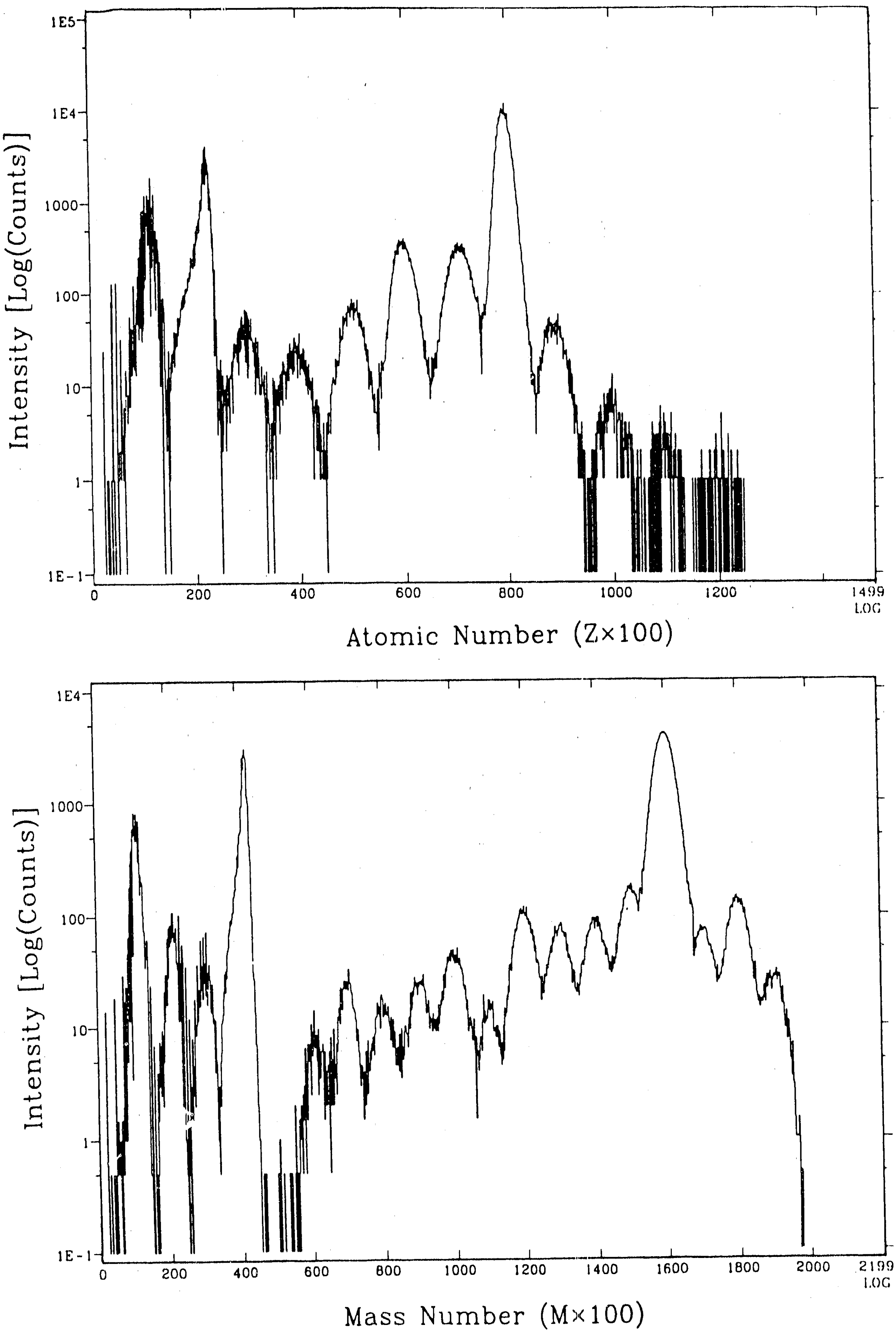
1E5
1E4
1000
100
10
1
1E-1
0
200
400
600
800
1000
1200
1499
LOG
Intensity [Log(Counts)]
Atomic Number (Z×100)
1E4
1000
100
10
1
1E-1
0
200
400
600
800
1000
1200
1400
1600
1800
2000
2199
LOG
Intensity [Log(Counts)]
Mass Number (M×100)

Fig. 3

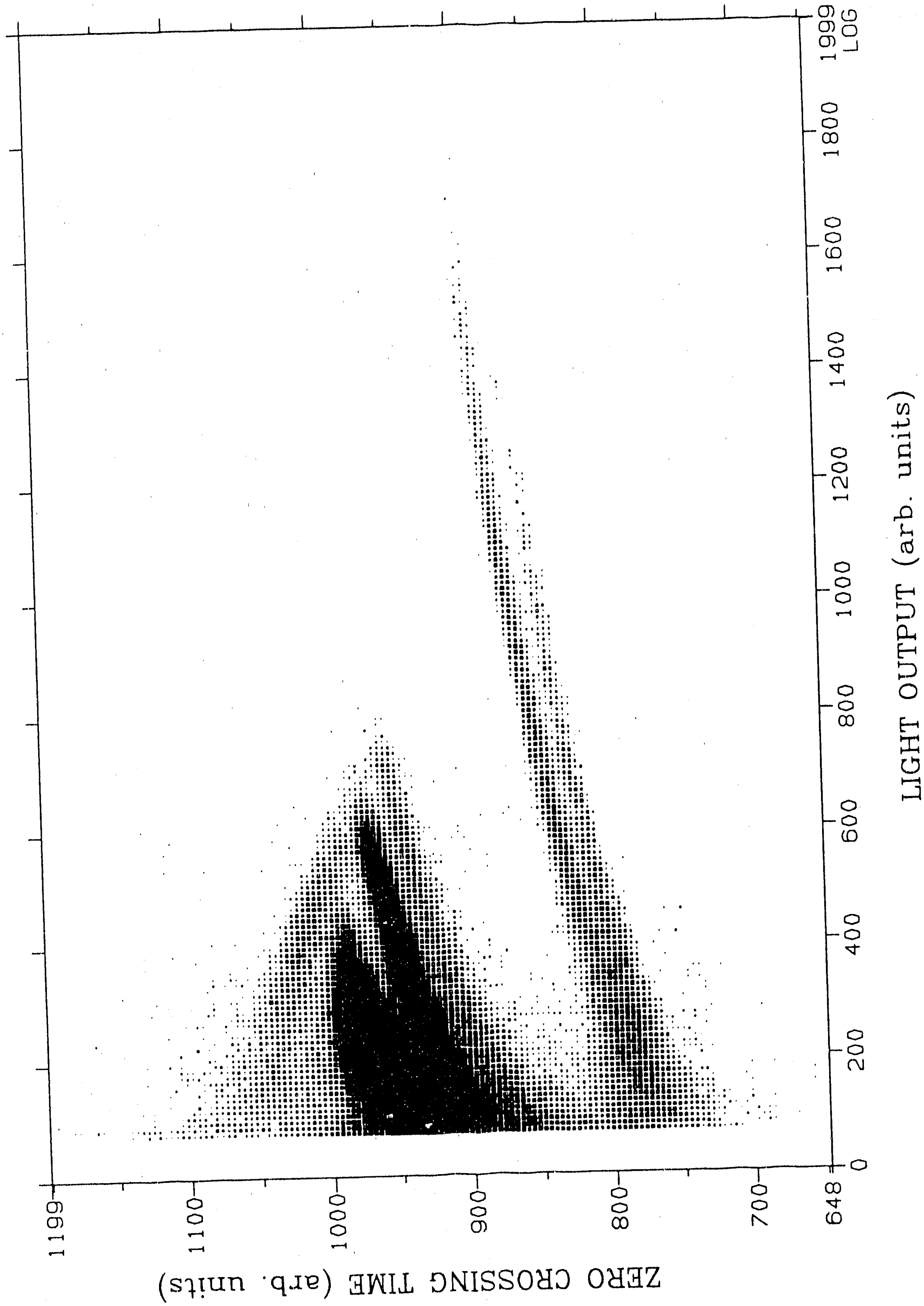
LIGHT OUTPUT (arb. units)
0
200
400
600
800
1000
1200
1400
1600
1800
1999
LOG
ZERO CROSSING TIME (arb. units)
648
700
800
900
1000
1100
1199

Fig. 4

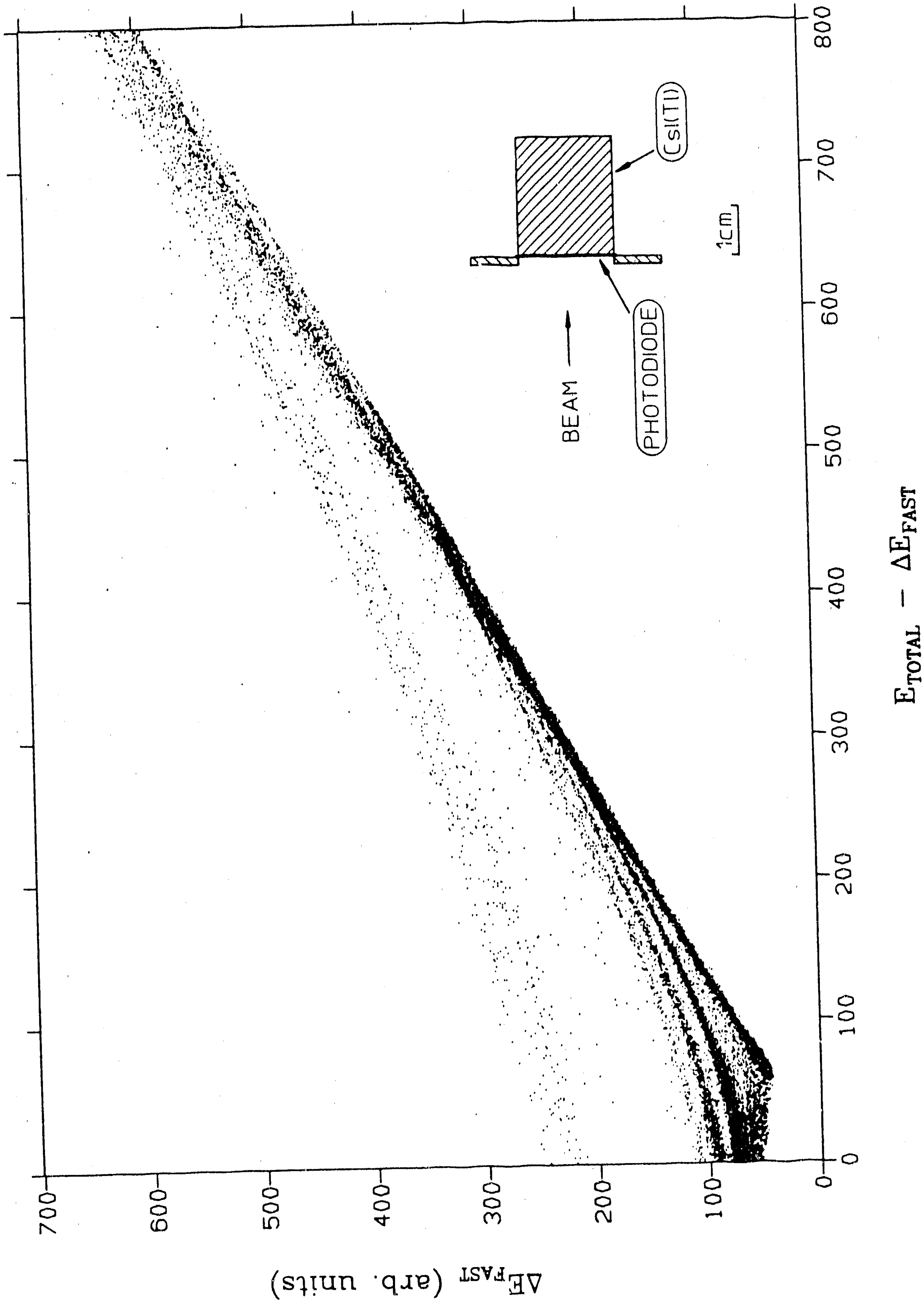
ΔE_FAST (arb. units)
E_TOTAL − ΔE_FAST
BEAM
PHOTODIODE
CsI(Tl)
1cm
0
100
200
300
400
500
600
700
800

Fig. 5

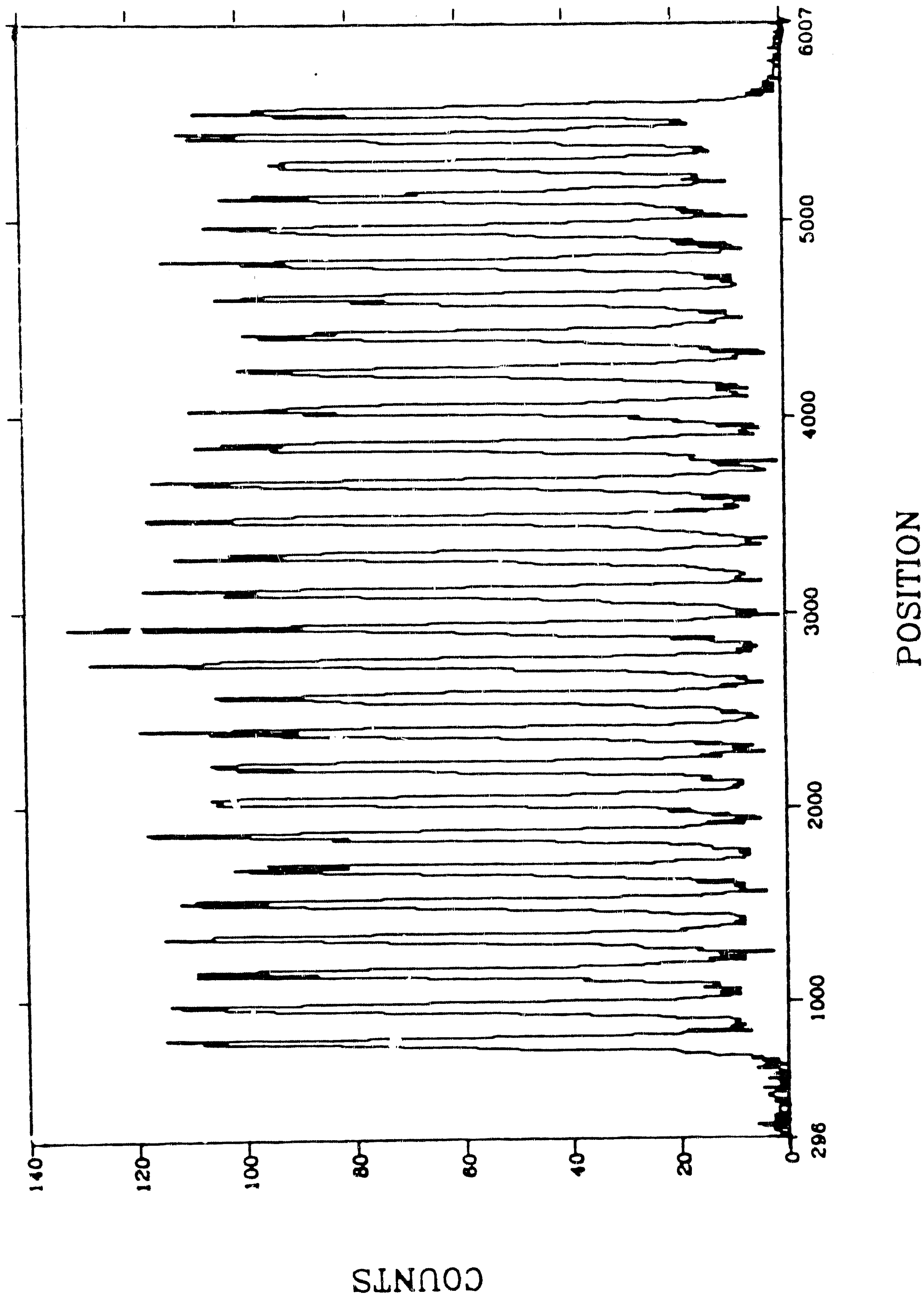
COUNTS
0
20
40
60
80
100
120
140
POSITION
296
1000
2000
3000
4000
5000
6007

Fig. 6

END

DATE FILMED

12 / 19 / 90